Spatial-temporal regulation improves the sensitivity and accuracy of synaptic vesicle recycling assays

Hansang Cho[1], Samuel V. Alworth[1], Seho Oh[1], Yuki Cheng[1], Brooke G. Kelley[2], Jane M. Sullivan[2] and James S.J. Lee[1]. [1]SVision LLC, Bellevue, WA 98006. [2]Department of Physiology and Biophysics, University of Washington, Seattle WA 98195.

Introduction

Enabled by newly available molecular probes and advanced microscopes, quantitative image based synaptic vesicle recycling assays using time-lapse digital imaging have become invaluable to basic research. There is broad interest in adapting these assays to a high throughput imaging format for applied research applications (e.g chemical genomics, drug discovery). This requires automated image recognition software to detect and define labeled axon terminals in the experimental images, extract the raw fluorescence measurements and perform kinetic modeling to estimate the time constant of vesicular reuse (τ). The achievable sensitivity of axon terminal segmentation and accuracy of measurement extraction and subsequent τ estimation is limited by the often weak and unstable signal received from the fluorescently labeled molecules, subject to image noise and variations from illumination, focusing and temporal movement. This represents a significant challenge to the analysis algorithm and therefore limits the quality of assay outcomes.

In this study, we have developed and validated novel and robust software methods of spatial-temporal regulation (STR) that enhance image signal and reduce image noise and variations to improve the quantitative analysis of synaptic vesicle recycling. The STR methods utilize the spatial-temporal signal consistency to improve axon terminal detection, measurement extraction and τ estimation. The current study results show that STR improves axon terminal detection sensitivity and specificity, axon terminal segmentation accuracy, and τ estimation accuracy across all levels of simulated noise.

Materials and Methods

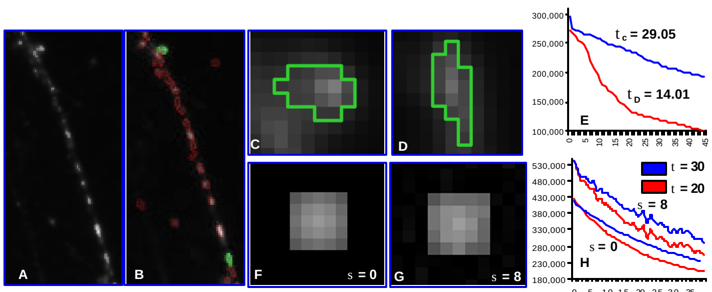

Fig 1. Real images and simulated image sets were used in the study. Study set consist of (i) a set of synaptic vesicle recycling movies using FM 4-64 (84 movies) **(A - E)**, (ii) four sets where noise from a zero mean Gaussian distribution with four different standard deviations was added to these recycling movies (336 movies), (iii) two sets of sixteen simulated movies where the individual synthetic synapses are destained with a known τ wherein (iv) one set's synthetic synapses are subject to a random sub-pixel shift (32 movies), and (v) five sets of images where five levels of zero mean Gaussian noise was added to the simulated movies (160 movies) **(F – H)**. Half of the movies of synaptic vesicle recycling and associated noise-added were separated into a training group (210 movies), and half into a testing group (210 movies) by stratified sampling. The training group was used for algorithm development and the testing group for performance evaluation.

Fig 2. Confidence maps used for regulation. Our STR methods make use of confidence maps rather than conventional binary segmentation masks. Spatial and temporal information from the entire movie can be used to adjust the confidence weighting at the individual pixel level to improve the noise immunity of the automated analysis. **(A)** Original image grayscale intensity values reveal an axon terminal labeled with FM dye. **(B)** Binary masks make a crisp on / off association of pixels to objects. **(C)** In contrast, confidence maps make a probabilistic association of pixels to objects using a confidence function. Non-binary, the confidence map encodes a confidence score between 0 and 255.

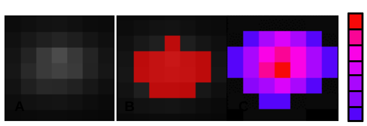

Fig 3. Spatial regulation. A spatial confidence algorithm is applied to a binary mask output of a segmentation algorithm to assign initial confidence map values. The algorithm is described in figure 3 and consists of: 1) Smooth image intensity: This step smoothes the image intensity by using a 5X5 average filter. 2) Get minimum and maximum intensity: This step determines the minimum (min) and maximum (max) intensity in a 5X5 dilated mask area of each object. 3) Confidence by standardization: This step creates initial confidence by normalization using the minimum and maximum values.

$$Confidence = 255 * \frac{I - \min}{\max - \min}$$

4) Confidence refinement by normalization: This step calculates intensity at the 75 percentile inside the segmentation mask (I_L). The confidence is normalized by I_L using the following:

$$Confidence^* = Confidence * \frac{255}{I_L}$$

5) Confidence conditioning: This step conditions the confidence by setting the value to zero at the mask corner when Avg(mask,3x3) < 128. The spatially regulated segmentation algorithm performed well in the test set movies and was tested without any change in parameters.

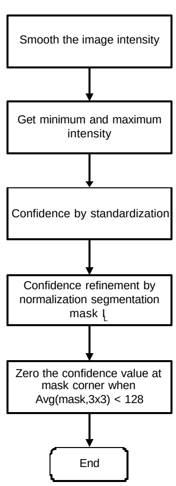

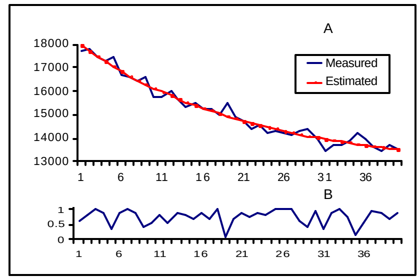

Fig 4. Temporal Regulation. We derived and implemented a nonlinear regression method for the constrained estimation of the exponential dissociation model parameter τ. The temporal confidence function improves the τ estimation by adjusting the confidence map values based on their temporal reliability. Multiple iterations of model fitting refinements progressively reduce the effect of data variation and thereby increase the accuracy and repeatability of the model fitting result. The figure **(A)** shows an example of measured data and the estimated τ curve for a synthetic object from a simulated image with noise σ = 4. **(B)** Shows the weights calculated for each time point.

Results

Table 1. Spatially regulated segmentation is more sensitive, specific and accurate than benchmark. The spatially regulated segmentation result was compared against a benchmark segmentation algorithm to establish a sensitivity, specificity and segmentation accuracy baseline for our approach. Results show that spatially regulated segmentation performed better than the benchmark with statistical significance in all tests. **(A)** Detection sensitivity for spatially regulated confidence map (test) and benchmark segmentation method. **(B)** McNemar test results for detection sensitivity: ?2 values and b/a ratios as well as p values at all noise levels. **(C)** Positive predictive value of test and benchmark segmentation. **(D)** McNemar test results for positive predictive value. ?2 values and b/a ratios as well as p values are provided at all noise levels. **(E)** Segmentation error comparison of test and benchmark methods including p values.

A

Noise	N0	N2	N4	N5	N6
Test	0.7089978	0.6336257	0.5685571	0.5636896	0.5698260
Benchmark	0.5012640	0.4844618	0.4574763	0.4681318	0.4404357

B

McNemar test result (sensitivity)	N0	N2	N4	N5	N6
χ2	3297.77	1943.88	1632.60	1675.09	1536.48
P value	< 0.001	< 0.001	< 0.001	< 0.001	< 0.001
b/a ratio	1.954	2.371	2.229	2.259	2.148

C

Noise	N0	N2	N4	N5	N6
Test	0.9382240	0.7269147	0.5707294	0.5228258	0.4857612
Benchmark	0.8554916	0.7234003	0.5435331	0.4867857	0.4362422

D

McNemar test result (PPV)	N0	N2	N4	N5	N6
χ2	421.39	0.8898	91.39	117.64	232.57
P value	< 0.001	< 0.5	< 0.001	< 0.001	< 0.001
b/a ratio	0.44	0.97	0.79	0.75	0.60

E

Noise	N0	N1	N4	N5	N6
Test	0.1615	0.2339	0.2681	0.2687	0.3322
Benchmark	0.4178	0.4180	0.4130	0.4124	0.4139
Paired sample T test p value	3.06e-33	1.33e-37	2.01e-15	2.44e-15	1.09e-12

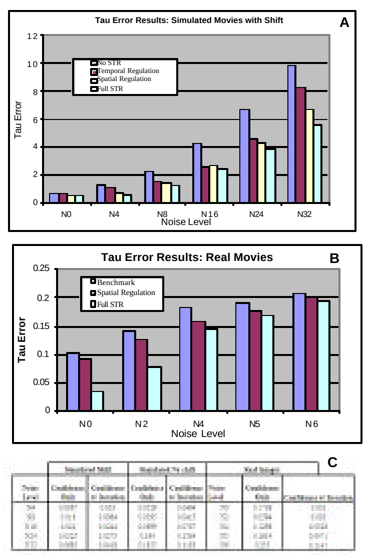

Fig 5. τ estimation accuracy study results. τ error was analyzed for (i) baseline (binary) method not subject to spatial or temporal regulation, (ii) test method subject to spatial regulation only, (iii) test method subject to temporal regulation only, and (iv) test method subject to spatial and temporal regulation using both simulated and real image sets. The results in **(A – C)** show that spatial regulation alone improves τ estimation and is more robust to noise with statistical significance. Adding temporal regulation can further increase the τ fitting accuracy. **(A)** shows the results for the 16 simulated with shift movies across 6 noise levels. **(B)** shows the results for the 42 real moves across five noise levels. Performance from spatial temporal regulation method is compared against performance using our segmentation with no STR. **(C)** compares spatial regulation, spatial and temporal regulation, and no regulation outcomes. The p-values are calculated from a t-test comparing τ error results of the non regulated test method to both the spatial regulation only, and spatial and temporal regulation methods using simulated movies (16 movies), simulated with sub-pixel shift movies (16 movies), and real movies test sets (42 movies). Spatial regulation only based improvements using real data have higher p values, but a combination of the spatial and temporal regulation can clearly reduce the error with statistical significance. The improvements delivered by spatial temporal regulation are significant for all but the highest noise level.

Conclusion

We have developed and validated novel image recognition methods which make use of the spatial temporal time-lapse image content to enhance the image signal and reduce image noise and variations to improve the quantitative analysis outcomes. We validated these spatial temporal regulation methods using time-lapse image sets from an FM dye-based assay of synaptic vesicle recycling, as well as synthetically created time-lapse movies. We found that the STR methods provide significant improvements in axon terminal detection sensitivity and specificity, axon terminal segmentation accuracy and τ fitting accuracy for both normal, simulated, and noise-added conditions.

We believe the methods of spatial and temporal regulation validated here for the synaptic recycling assay provide a good baseline for subcellular time-lapse assay analyses, and could be applicable to a broad range of subcellular assays.

We are grateful to Greg Martin of the University of Washington, Keck Imaging Center who helped select and design the benchmark segmentation algorithm. This work was supported in part by grant number 1R43MH075498-01 from the National Institute of Mental Health